Double dendrite growth in solidification

Brian Utter* and E. Bodenschatz
Laboratory of Atomic and Solid State Physics, Cornell University, Ithaca, New York 14853, USA
(Received 10 March 2004; revised manuscript received 4 April 2005; published 7 July 2005)

We present experiments on the doublon growth morphology in directional solidification. Samples used are succinonitrile with small amounts of poly(ethylene oxide), acetone, or camphor as the solute. Doublons, or symmetry-broken dendrites, are generic diffusion-limited growth structures expected at large undercooling and low anisotropy. Low anisotropy growth is achieved by selecting a grain near the {111} plane leading to either seaweed (dense branching morphology) or doublon growth depending on experimental parameters. We find selection of doublons to be strongly dependent on solute concentration and sample orientation. Doublons are selected at low concentrations (low solutal undercooling) in contrast to the prediction of doublons at large thermal undercooling in pure materials. Doublons also exhibit preferred growth directions and changing the orientation of a specific doublonic grain changes the character and stability of the doublons. We observe transitions between seaweed and doublon growth with changes in concentration and sample orientation.

DOI: 10.1103/PhysRevE.72.011601 PACS number(s): 68.70.+w, 81.30.Fb

I. INTRODUCTION

Over the past 20 years, surface tension anisotropy has been discovered to be fundamental in determining solidification morphology. Perhaps the greatest success was the discovery that anisotropy is required for the formation of stable cells and dendrites through a microscopic solvability condition [1]. In contrast, an isotropic surface tension leads to complicated, tip splitting growth known as dense branching morphology [2] or seaweed growth [3] [e.g. Fig. 1(B)]. This is a generic feature of diffusion limited growth and exists in a variety of systems under isotropic or weakly anisotropic conditions, such as viscous fingering, bacterial colony growth, and electrodeposition [4].

It was predicted by Brener *et al.* for the solidification of a pure material that a transition from fractal to compact (nonfractal) seaweed occurs with increasing undercooling Δ [5]. This morphology diagram, reproduced in Fig. 2, also shows transitions between meandering seaweed growth (S) and ordered dendritic growth (D) with increasing anisotropy ϵ. For a pure material, thermal undercooling (Δ) increases with growth speed for both dendrites and doublons, so the vertical axis can be thought of as growth velocity (V). At low growth speeds, perturbations at the tip lead to tip splitting and fractal geometries while at higher speeds they convect away, producing compact growth [5]. The basis of the higher speed growth (compact seaweed) is the doublon, or symmetry-broken dendrite, in which two asymmetric cells grow cooperatively such that there is a parabolic envelope over the pair of cells and a thin liquid gap of well-defined size separating them [6]. An example of this is shown in Fig. 1(A), where three stable doublons in a compact seaweed growth front are shown. It is somewhat counterintuitive to observe random, fractal seaweed patterns at low driving force (V) and oriented doublon growth at large driving force. The isotropy in surface tension is revealed in that although doublons have a clear orientation as they grow, it is expected to be randomly selected in the isotropic case [5].

Stable "parity broken cells" were first observed numerically by Brener *et al.* [7] and Ihle and Müller-Krumbhaar [3]. Since the early observation of an array of "doublets" by Jamgotchian *et al.* [8], they have attracted significant interest. The existence of doublons was noted in eutectic growth by Kassner *et al.* [9]. Subsequent simulations [10,11], theories [12,13] and experiments [14–16] have probed their stability, characteristics and formation. In particular, Losert *et al.* [14] imposed periodic perturbation experimentally to test doublon stability. In their work, they didn't find doublons appearing without an imposed perturbation except as transients.

The morphology diagram of Brener *et al.* [5] (Fig. 2) describes the expected growth as surface tension anisotropy and undercooling are changed. Although it is assumed to be a general phase diagram, the boundaries separating different types of growth are determined for the solidification of a pure material, so no explicit dependence on solute concentration is known for doublon growth in binary alloys. Solute concentration does affect the undercooling [1] and must be included for a proper analysis of solutal doublons. Solutal undercooling is proportional to sample concentration

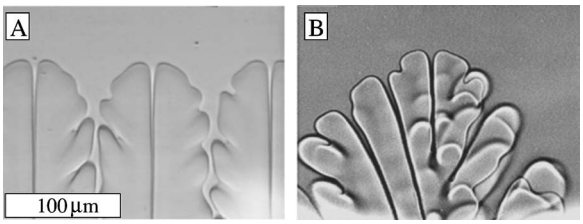

FIG. 1. (A) Stable doublons in a compact seaweed growth front in 0.5% PEO-SCN at a growth rate V=22 μm/s. (B) Seaweed growth in 0.25% PEO-SCN at the same growth rate. A transient doublon develops before breaking apart.

*Electronic address: utterbc@jmu.edu

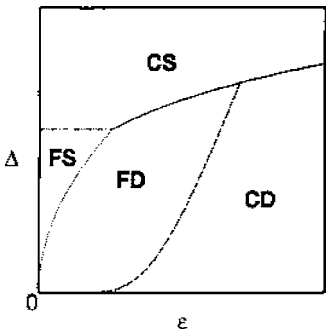

FIG. 2. Morphology diagram of Brener *et al.* [5] showing expected growth morphologies with changes in anisotropy (ϵ) and undercooling ($\triangle$). The morphologies identified are fractal seaweed (FS), compact (nonfractal) seaweed (CS), fractal dendrite (FD), and compact dendrite (CD).

$[=mC_\infty(1-k)/k$, where m is the liquidus slope, C_∞ is bulk sample concentration, and k is the partition coefficient].

Direct comparisons using different cells to study concentration and crystal orientation effects can be difficult because of variations between the cells in sample thickness, crystal orientation, and possible solute segregation. For instance, Figs. 1(A) and 1(B) show growth in two sample cells of different thickness and unknown grain orientation, so we cannot directly conclude the differences due specifically to concentration.

In this article, we isolate the effects of concentration and crystalline orientation on the stability of solutal doublons. We focus on concentration effects by slowly growing a grain halfway through a cell, effectively zone-refining a region of the sample to produce a step in concentration. We then grow a single crystal through the cell to study the sudden increase or decrease in concentration on a particular grain in a single cell. We study orientation effects by observing a single grain in a sample cell that we can rotate between runs. We also study the expected transition from fractal seaweed to compact seaweed (doublon) growth with increasing growth rate. We find below that for a given grain and growth speed, doublons are preferred at low solute concentrations (small solutal undercooling) rather than at large undercooling as expected in Fig. 2 for thermal doublons. We also find that doublons in directional solidification are not isotropic and have a particular orientation. The specific sample orientation affects the existence and character of the doublons.

II. EXPERIMENTAL TECHNIQUES

The experimental apparatus used presently has been described previously [17] and additional details will be presented elsewhere [18]. We perform experiments with a traditional directional solidification apparatus in which a quasi-two-dimensional sample ($13\ \text{cm} \times 1.5\ \text{cm} \times (5-60)\ \mu\text{m}$) is pulled through a linear temperature gradient at a constant pulling velocity. After an initial transient, the average speed of the solidification front is equal to the pulling speed, set by a linear stepping motor with 4 nm step size.

The cell consists of two glass plates glued together and filled with the sample. The glass plates are cleaned in stages using detergent, acetone, methanol, an acid solution (sulfuric acid and NoChromix), and distilled water. The glue used is the epoxy Torr-Seal. The nominal cell depth is set by a Mylar spacer.

TABLE I. Properties of samples used in this study. Succinonitrile alloys with acetone, camphor and poly(ethylene oxide) as solutes. Diffusivity D, partition coefficient k, solute concentration $C(\pm 0.02\%)$, and sample thickness $d(\pm 2\ \mu\text{m})$ also listed. (a) From [20]. (b) From [21]. (c) From [22].

	ACE-SCN	CAM-SCN	PEO-SCN
D ($\mu\text{m}^2/\text{s}$)	1270[a]	300[b]	80
k	0.1[a]	0.33[c]	0.01
C (wt. %)	1.5%	1.3%	0.25%
d (μm)	20	22	60

In each set of runs, we maintain the temperature gradient G at a fixed value between 3 and 50 K/cm with a stability of ± 2 mK. The temperatures of the hot and cold sides are above and below the equilibrium melting temperature of $\approx 58\ ^\circ\text{C}$ so that the solid-liquid interface remains within the gap between the temperature controlled blocks. It is also possible to rotate the cell within the sample plane between runs. This allows for control over in-plane sample orientation.

The sample used is a model alloy of succinonitrile (SCN) and a small amount of added solute. The solutes used in this study are either 0.25% poly(ethylene oxide) (PEO) [19], 1.5% acetone (ACE), or 1.3% camphor (CAM). The diffusivities D and partition coefficients k are listed in Table I with the solute concentrations C and sample thicknesses d.

We purify succinonitrile using a vacuum distillation apparatus. Mixing with solute is performed under inert argon atmosphere. Samples are filled using a vacuum filling technique in order to degas the sample and prevent contamination [18].

We observe the liquid-solid interface with phase contrast or Hoffman modulation contrast microscopy. Sequences of images are recorded using a CCD camera with a framegrabber or time lapse video.

To initiate growth, we melt the sample completely and quench it, seeding a number of grains. We select one grain with the desired orientation and all others are melted off so the chosen grain can grow and fill the width of the cell. To have a nearly isotropic effective surface tension within the growth plane, the chosen grain must be near the {111} plane [6]. Before each run, the sample is kept stationary ($V=0$) for a sufficient time to equilibrate.

III. RESULTS

Our early observations of doublons confirmed the fact that they are generally unstable to tilting [6]. Doublons that appear to be growing straight will eventually begin leaning towards one side and the cell on that side will suddenly be convected away. The remaining cell then splits to form another transient doublon. The tilting instability generally repeats on the same side since a small amount of crystalline

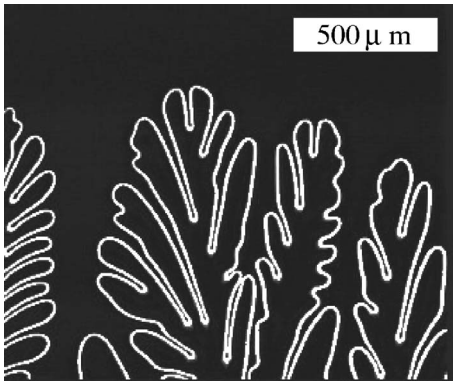

FIG. 3. Degenerate seaweed at low growth speed. The initial tip splitting appears similar to the process of doublon formation. The sample is 0.25% PEO-SCN at V=2.71 μm/s and G=18 K/cm.

anisotropy usually breaks the symmetry. In one of our first efforts to study doublon formation, we examined the degenerate seaweed described previously [17,23]. At higher growth velocities, we do find the expected doublonic structures, but they are often intermittent and short-lived. As a doublonic dendrite forms, there are initially two asymmetric cells with a characteristic gap of well defined thickness as in Fig. 1(B). Although there is not a parabolic envelope over the tips, they are clearly asymmetric with the tips closer together than the cellular spacing and the gap appears to be well selected.

Doublons are predicted to be the basis for seaweed growth, so it is no surprise that the same description of the tilt instability could be given of seaweed tip splitting. During the tip splitting of seaweeds, the cell briefly appears as a pair of asymmetric cells as in Fig. 3. This is the same grain as in Fig. 1(B) at a lower growth speed. The gap h between the fingers is also quite regular. To show this more clearly, in Fig. 4(A), the interface near the tip region has been extracted in subsequent images and displaced upwards a distance $V\Delta t$ where Δt is the time interval between pictures, i.e., this is an image in a frame where the tip grows upwards at speed V. There we see that the initial gap between seaweed lobes is clearly selected, as with doublons. In Fig. 4(B), the gap thickness is measured for seaweeds at different pulling

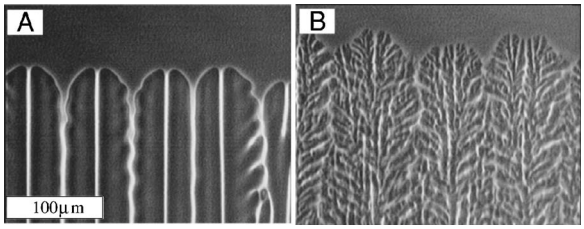

FIG. 5. Doublon to seaweed transition with an increase in concentration. The same grain is grown from (A) a zone refined (low concentration) into (B) a bulk (high concentration) region of the same cell. The sample is CAM-SCN at V=86.4 μm/s and G =40 K/cm.

speeds. The gap thickness scales approximately as $h \propto V^{-0.5}$. The scaling for the seaweed gap thickness is consistent with the $\lambda \propto V^{-0.5}$ scaling found for fingering wavelengths in solidification [24] and inconsistent with the prediction of $h \propto V^{-7/9}$ for doublons [5]. The discrepancy could indicate that the seaweed tip is not strictly a transient doublon and that doublons are not the fundamental building blocks of seaweed growth. However, we are not able to verify the 7/9 exponent for the solutal doublons we observe, since the resolution of our images is not sufficient to resolve the doublon gap thickness.

We find the stability of doublons to be strongly concentration dependent. In a seaweed grain showing unstable doublons, we allowed a flat interface to grow at small pulling speeds, effectively zone-refining a section of the cell. After backing up and growing through the zone refined area and into a region of higher concentration, we observe stable doublons which break apart into unstable seaweed structures as the solute concentration increases, as in Fig. 5. This is repeatable for the different mixtures used in this study. In one case, we then rotated the cell 180° and forced the grain to grow from a region of high concentration to low concentration and saw the opposite transition from unstable seaweeds to stable doublons. The latter transition is shown in Fig. 6. Note that since the average interface position is at a higher melting temperature for lower solute concentration, the camera is moved along the growth direction and the relative thermal undercooling cannot be determined directly from these images.

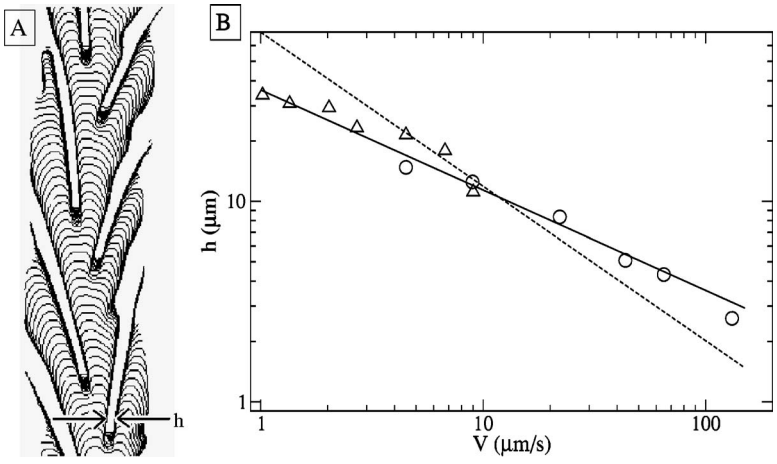

FIG. 4. The evolution of the tip region over time is shown on the left. The regularity of the gaps suggests doublon formation. The gap thickness h is plotted versus pulling speed for (△) PEO-SCN and (○) ACE-SCN. The solid line shows $h \propto V^{-0.5}$. Fitting the exponent gives (△) -0.45 ± 0.05 and (○) -0.52 ± 0.05. This compares to Brener *et al.*'s predicted exponent for doublons ($h \propto V^{-7/9}$, dashed line).

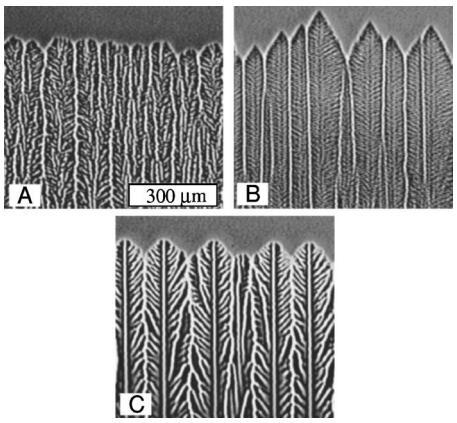

FIG. 6. (A) Seaweed to (C) doublon transition with a decrease in concentration. During this transition, the interface rapidly advances, forming (B) transient superdendrites before forming doublons. The sample is CAM-SCN at $V \approx 150$ μm/s and $G = 18$ K/cm.

In the seaweed to doublon transition, since the interface must advance quickly towards a new equilibrium interface location as the concentration decreases, we see transient superdendrites, shown in Fig. 6(B). These are triangular growths that commonly form at large growth velocities [25]. The progression is counter to what might be expected from Brener *et al.*'s morphology diagram. At lower concentration, the interface advances to lower undercooling, so we might expect a transition from doublon to seaweed growth, contrary to our observations. However, as mentioned earlier, the morphology diagram is discussed in the context of a pure sample and may not be applicable with concentration changes. We show a second example of the seaweed to doublon transition in Fig. 7.

It is interesting to note that the unstable seaweed growth in each case still maintains a coarse spacing that is similar to that for the doublons. The doublons we observe though are not alternating shallow and deep grooves as in [14]. Particularly in Fig. 7(B), we see dendritic doublons with much more strongly developed sidebranches than most previous observations [6].

At low concentrations, doublons appear to be stable and rarely undergo the tilting instability described above. Doublons appear to be strongly selected without an imposed modulation (e.g., Fig. 5) unlike what is reported by Losert *et al.* [14].

In numerical simulations, higher noise deters doublon growth [14]. The relevant noise in our system is most likely

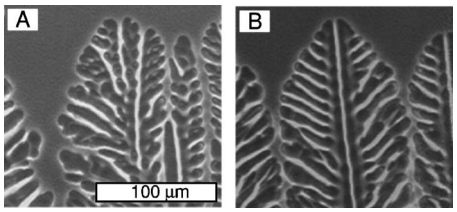

FIG. 7. Seaweed to doublon transition with a decrease in concentration. The sample is CAM-SCN at $V \approx 150$ μm/s, and $G = 18$ K/cm.

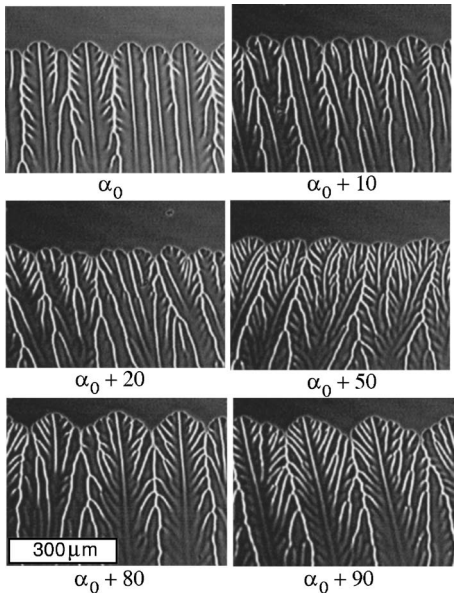

FIG. 8. Doublon growth with changes in orientation. A grain showing doublon growth shows transient doublons when rotated counterclockwise by 10° and essentially no doublon formation at higher rotation angles. The sample is 0.5% PEO-SCN at $V = 86.4$ μm/s.

concentration fluctuations rather than the thermal noise relevant in growth of pure materials. In this case, higher concentrations would then correspond to larger fluctuations and larger noise. It is also possible that the surface tension changes with concentration [26] which could lead to a change in morphology. This seems plausible because higher concentrations (and thinner samples) lead to seaweed growth more readily than dendritic growth, particularly when using PEO as solute.

We also observe an orientational dependence of doublon growth. It is believed that for completely isotropic systems, doublons will spontaneously select a growth direction since none is preferred [5]. However, Losert *et al.* report that no stable doublons are found for zero anisotropy in simulations [14]. In our experiments, anisotropies are clearly present and lead to a preferred doublon orientation. Figure 8 shows the results of an experiment in which the cell can be rotated within the sample plane in order to further probe the effect of crystal orientation on growth. The arbitrary angle α_0 reflects the fact that we know relative angles as the sample is rotated rather than absolute crystallographic orientations. We see that doublons are oriented along particular directions and their stability depends on orientation. In particular, doublons are more stable when oriented along a favored growth direction. One explanation for this is that the tilt instability described above is more prevalent for tilted doublons. We also note that the crystalline anisotropy need not be fourfold symmetric as is often assumed [17].

The long-time behavior of doublon growth can be seen in Fig. 9, which shows a space-time plot for doublons shown in Fig. 1(A). This is essentially a chart recording of the growth and is created by extracting lines at a fixed distance behind the interface for sequential pictures (see [6], for example).

FIG. 9. Space-time plot of doublon growth in 0.5% PEO-SCN at $V=22$ μm/s. This run corresponds to the sample shown in Fig. 1. The dark central line indicates the inner groove of a doublon as it meanders in the field of view. The image width is 243 microns and the time of 48 seconds increases upwards.

The central gap of the doublon is identified by the dark line. Although we observe a doublon tip growing for over 48 seconds (in a run of several minutes), it meanders over time. This is different from the oriented growth of dendrites which typically grow along fixed, preferred directions at steady-state. Doublons in this regime are also eliminated through the tilt instability, but their lifetime is significantly longer. The gap between fingers is observed to be very uniform over time. The positions of the tips of the asymmetric pair along the growth direction is also equal within the resolution of our data. Therefore, we are not able to test Müller-Krumbhaar *et al.*'s suggestion for the mechanism of doublon stability [27] in which if one finger grows ahead, it has more room and widens, leading to a lower growth velocity.

Figure 10 shows doublonic dendrites with sidebranches perpendicular to the sample plane. In this case, the sample thickness is large enough to support the transverse sidebranching mode. In three dimensions, the triplon is predicted to be the basic building block of isotropic growth [28], although transient doublons have been observed in 3D growth

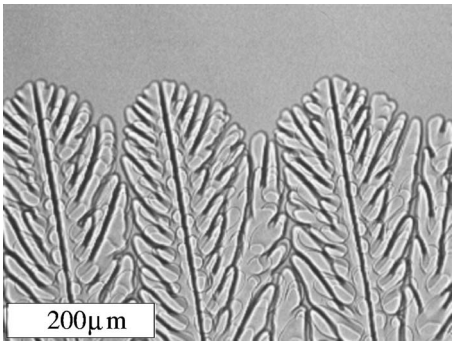

FIG. 10. Doublonic dendrites. Sidebranches perpendicular to the plane of growth are evident. The sample is PEO-SCN at $V=86.4$ μm/s.

of xenon dendrites [29]. If we were able to increase the thickness of the sample, we would expect a transition from the three-dimensional doublons in Fig. 10 to triplons, although the nature of the transition is unknown. In two dimensions, multiblons have been shown in numerical simulations and were argued to be generically unstable [11]. In our observations, multiblons can be seen as transients but are not found to be stable.

IV. CONCLUSIONS

In conclusion, we observe doublons in low anisotropy growth but they are often unstable to a tilting instability. We find doublon formation to be strongly dependent on solute concentration and sample orientation. Doublons are selected at low concentrations (small solutal undercooling) in contrast to the fact that doublons exist at large thermal undercoolings in pure materials. Perhaps the dominant factor is that larger concentrations lead to larger fluctuations which destabilize the tip. Doublons also exhibit a preferred growth direction and changing the orientation of a specific doublonic grain demonstrates that the character and stability of doublons depend on crystalline orientation. Even when stable, doublons tend to meander, unlike in dendrite growth. At higher concentrations and when the preferred growth direction is substantially different from the imposed growth direction, we observe the seaweed morphology. We observe seaweed-doublon transitions with changes in these parameters. In seaweed growth, the tip splitting process appears similar to the formation of transient doublons. However, the gap thickness h scales with the velocity V as $h \propto V^{-0.5\pm0.05}$ rather than $V^{-7/9}$ as predicted for doublons. This might indicate that seaweed growth should not strictly be viewed as composed of transient doublons. However, with the resolution of our images, we are not able to verify or reject the 7/9 exponent for the narrow gap thickness of solutal doublons.

It remains unclear what determines the stability of solutal doublons, particularly with changes in solute concentration. Doublons should also be observable in other systems if the assumed morphology diagram is generic. The effects of anisotropies or concentration in these systems are open questions.

ACKNOWLEDGMENTS

We would like to thank Rolf Ragnarsson for significant contributions in related work leading to these experiments. This work was supported by the Cornell Center for Materials Research (CCMR), a Materials Research Science and Engineering Center of the National Science Foundation (DMR-0079992).

[1] For reviews, see, for example, J. Souletie Langer, in *Chance and Matter*, edited by J. Souletie *et al.* (North-Holland, Amsterdam, 1987), pp. 629–711; Y. Saito, *Statistical Physics of Crystal Growth* (World Scientific, New Jersey, 1996).
[2] E. Ben-Jacob *et al.*, Phys. Rev. Lett. **57**, 1903 (1986).
[3] T. Ihle and H. Müller-Krumbhaar, Phys. Rev. Lett. **70**, 3083 (1993); Phys. Rev. E **49**, 2972 (1994).
[4] See, for example, K. McCloud and J. Maher, Phys. Rep. **260**, 139 (1995); T. Matsuyama and M. Matsushita, Crit. Rev. Microbiol. **19**, 117 (1993); E. Ben-Jacob, and P. Garik, Nature (London) **343**, 523 (1990).
[5] E. Brener, H. Müller-Krumbhaar, and D. Temkin, Phys. Rev. E **54**, 2714 (1996); E. Brener, H. Müller-Krumbhaar, D. Temkin and T. Abel, Physica A **249**, 73 (1998).
[6] S. Akamatsu, G. Faivre, and T. Ihle, Phys. Rev. E **51**, 4751 (1995).
[7] E. Brener, H. Müller-Krumbhaar, Y. Saito, and D. Temkin, Phys. Rev. E **47**, 1151 (1993).
[8] H. Jamgotchian, R. Trivedi, and B. Billia, Phys. Rev. E **47**, 4313 (1993).
[9] K. Kassner, A. Valance, C. Misbah, and D. Temkin, Phys. Rev. E **48**, 1091 (1993).
[10] R. Kupferman, D. Kessler, and E. Ben-Jacob, Physica A **213**, 451 (1995).
[11] P. Kopczynski, W.-J. Rappel, and A. Karma, Phys. Rev. E **55**, R1282 (1997).
[12] E. A. Brener and D. E. Temkin, JETP **82**, 559 (1996).
[13] M. Ben Amar and E. Brener, Phys. Rev. Lett. **75**, 561 (1995); Physica D **98**, 128 (1996).
[14] W. Losert *et al.*, Phys. Rev. E **58**, 7492 (1998).
[15] M. Georgelin and A. Pocheau, Phys. Rev. Lett. **79**, 2698 (1997).
[16] A. Ludwig, Phys. Rev. E **59**, 1893 (1999).
[17] B. Utter and E. Bodenschatz, Phys. Rev. E **66**, 051604 (2002).
[18] B. Utter, R. Ragnarsson, and E. Bodenschatz, Rev. Sci. Instrum. **76**, 013906 (2005).
[19] Poly(ethylene oxide) with an attached rhodamine dye [Sulferhodamine Bis-(PEG 2000), molecular wt. 4500] is purchased from Molecular Probes, Inc. (Eugene, OR).
[20] M. Chopra, M. Glicksman, and N. Singh, J. Cryst. Growth **92**, 543 (1988).
[21] T. Sato, W. Kurz, and K. Ikawa, Trans. Jpn. Inst. Met. **28**, 1012 (1987).
[22] T. Taenaka, H. Esaka, S. Mizoguchi, and H. Kajioka, Mater. Trans., JIM **30**, 360 (1989).
[23] B. Utter, R. Ragnarsson, and E. Bodenschatz, Phys. Rev. Lett. **86**, 4604 (2001).
[24] R. Trivedi and W. Kurz, Acta Metall. Mater. **42**, 15 (1994).
[25] R. Ragnarsson, B. Utter, and E. Bodenschatz, in *Phase Transformations and Systems Driven Far From Equilibrium*, edited by E. Ma (Materials Research Society, Warrendale, PA, 1998), Vol. 481, pp. 65–70.
[26] C. Charach and P. Fife, J. Cryst. Growth **198–199**, 1267 (1999).
[27] H. Müller-Krumbhaar, M. Zimmer, T. Ihle, and Y. Saito, Physica A **224**, 322 (1996).
[28] T. Abel, E. Brener, and H. Müller-Krumbhaar, Phys. Rev. E **55**, 7789 (1997).
[29] I. Stalder and J. Bilgram, Europhys. Lett. **56**, 829 (2001).